Journal of Structural Biology 172 (2010) 270–275

Contents lists available at ScienceDirect

Journal of Structural Biology

journal homepage: www.elsevier.com/locate/yjsbi

Keratin homogeneity in the tail feathers of *Pavo cristatus* and *Pavo cristatus* mut. alba

S. Pabisch [a], S. Puchegger [a], H.O.K. Kirchner [b], I.M. Weiss [b], H. Peterlik [a,*]

[a] University of Vienna, Faculty of Physics, Strudlhofgasse 4, A-1090 Vienna, Austria
[b] INM – Leibniz Institute for New Materials, Campus D2 2, D-66123 Saarbrücken, Germany

ARTICLE INFO

Article history:
Received 30 March 2010
Received in revised form 8 July 2010
Accepted 10 July 2010
Available online 15 July 2010

Keywords:
Beta-keratin
Peacock feather
Structure
X-ray diffraction

ABSTRACT

The keratin structure in the cortex of peacocks' feathers is studied by X-ray diffraction along the feather, from the calamus to the tip. It changes considerably over the first 5 cm close to the calamus and remains constant for about 1 m along the length of the feather. Close to the tip, the structure loses its high degree of order. We attribute the X-ray patterns to a shrinkage of a cylindrical arrangement of β-sheets, which is not fully formed initially. In the final structure, the crystalline beta-cores are fixed by the rest of the keratin molecule. The hydrophobic residues of the beta-core are locked into a zip-like arrangement. Structurally there is no difference between the blue and the white bird.

1. Introduction

Recently the evolutionary development of feathers, the transition from Reptilia to Aves, and the associated capacity of flying (Alexander et al., 2010; Benton, 2010; Ruben, 2010; Stone, 2010; Sullivan et al., 2010) have received some attention. The evolutionary question is paralleled by the chemical one, the dichotomy between "hard" alpha-keratin in mammalia, and "soft" feather beta-keratins in reptiles and birds (Eckhart et al., 2008). Concerning the nomenclature, there is some confusion in the literature. Astbury and Woods (1934) stretched alpha-keratin to what he called a beta-form. Obviously their alpha- and beta-keratins have the same chemical composition, differing only in structure like two phases under stress. The feather beta-keratin is chemically different, but gives similar diffraction patterns to Astbury's stretched alpha (Astbury and Marwick, 1932).

The increased interest in feathers in general has led (Weiss and Kirchner, submitted for publication) to investigate one particular type in one particular bird, the tail covert feathers of the peacock, both blue and white. The chemical, biochemical and mechanical differences between the blue and the white animal are but little. *Pavo cristatus* and *Pavo cristatus* mut. alba belong to the same species, the latter is a subspecies and not an albino form. White parents beget white offspring, blue parents blue offspring. The tail feathers are not used for flying but serve for sexual display. For that purpose they are long and thin, mechanically speaking they are slender beams. They consist of an outer cortex in the form of a circular hollow self-similar cone, filled by a low density foam, the medulla. Both are made of the same keratin, which is subsequently called peacock keratin. In what precise sense this is identical to commonly called beta-keratin or not, is a delicate question (Dalla Valle et al., 2007). Chemically however, (Weiss and Kirchner, submitted for publication) have ascertained that the composition of our peacock keratin is identical to the F-keratin from *Larus novae-hollandiae* (Silver gull) (O'Donnell and Inglis, 1974). Polarized light microscopy, Fig. 1, reveals that the cortex is not uniform in the radial direction, but is a multilayer structure. This has been anticipated on the diffraction level by Busson et al. (1999).

Each such feather (Fig. 2A) of about 2 mm diameter at the base and 1 m length is produced once a year, amounting to a production rate of about 1 cm/day during the winter–spring growth period. The diameter of the feather keeps increasing (Fig. 2B), which amounts to ever increasing production volumes per day. Although the geometry changes considerably, the quality of the material produced remains surprisingly uniform. Weiss and Kirchner (submitted for publication) showed that Young's modulus of the cortex varies at most ten percent between tip and calamus, say between November and March. The purpose of this note is to check how the mechanical constancy is based on structural constancy. Is the keratin and its structural arrangement the same between tip and calamus? Does the diffraction pattern change? The structure of the feather keratin molecule is not perfectly known. Moreover, the arrangements of the crystallized β-sheets (Fraser and Parry, 2008) concerns from proline to proline only 31 amino acids (3.3 kDa) of the 98 amino acids (9.8 kDa) of the entire molecule. If, and how the rest of the molecule, after all two thirds and consisting of a 20 amino acids long N-terminus and a 47 amino acids long C-terminus, are crystallized and leave a mark on the diffraction pattern has remained open to speculation.

* Corresponding author.
E-mail address: herwig.peterlik@univie.ac.at (H. Peterlik).

1047-8477
doi:10.1016/j.jsb.2010.07.003

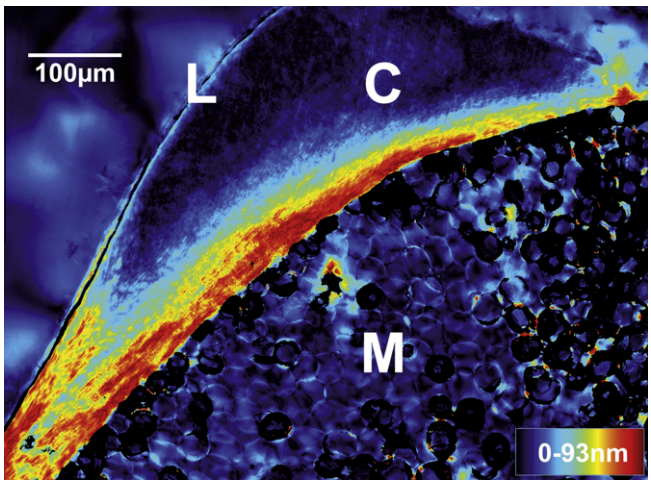

Fig. 1. Polscope (Cri Abrio System, L.O.T. Oriel, Germany) image of a rachis cross-section. Below the diagonal the foamy medulla structure (M) can be seen. It is surrounded by the cortex (C) of varying thickness, appearing moon-shaped. This is sub-structured into layers. Towards the top left, the cortex is covered by protective, presumably lipid, layer (L). Birefringent retardation (0–93 nm) is color coded.

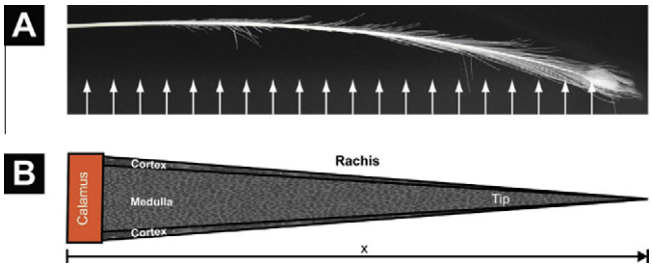

Fig. 2. (A) The tail cover feather of *Pavo cristatus* sub. alba subjected to X-ray investigation. The arrows indicate approximately the multiple beam positions. (B) Sketch of the conical shape of the rachis. Both outer diameter and cortex thickness decrease linearly from the calamus to the tip, forming a self-similar cone filled by the medulla. Diffraction patterns were taken from the cortex only.

Avian feathers are strongly textured, the axes of the fibrous protein and of the rachis being parallel. Early X-ray diffraction favoured an arrangement of pleated sheats (Astbury and Beighton, 1961) with a helical structure (Schor and Krimm, 1961a,b). The structure of the molecule was identified from X-ray diffraction patterns of a seagull feather (Fraser et al., 1971) as a helical arrangement of four repeating units per turn with a pitch length of 9.5 nm. Two twisted β-sheets are aligned along a perpendicular diad in a left-handed way, whereas the twist in the sheets is opposite to the one of the helix (Fraser et al., 1971). Fraser and Parry (1996) showed that within each β-strand a well-defined oscillation in hydropathy exists, which is consistent with the residues alternating between inner and outer surfaces of the residues. These authors refined the original model and proposed two possible configurations for hairpin turns in the β-sheets and a high concentration of hydrophobic residues in the interface between the sheets related by the diad (Fraser and Parry, 2008). In one of the models, there is a strong interaction of the two components within the helix with a smaller distance of arginine sidechains of only 0.4 nm, whereas in their complementary model the distance is 0.68 nm (Fraser and Parry, 2008). Due to this smaller distance, which facilitates dimerization, they favoured the first model, but they concluded that a stabilizing influence from the formation of disulfide linkages is rather unlikely as the cysteine residues are not close enough. The longitudinal texture of swan, goose, and ostrich feathers was studied by synchrotron radiation along the feather from the calamus to the tip (Cameron et al., 2003). The observed decrease of half-width of three specific reflections (i.e. a higher axial alignment of the keratin molecules with respect to the feather axis) was related to an increase of the Young's modulus for the two flying birds (Cameron et al., 2003). This was the starting point for the present work. We focus on a precise determination of the structure along the length of a peacock's feather, between the calamus and the tip with the eye of the feather.

2. Experimental

The tail covert feathers of a white and a blue peacock were obtained commercially (Claude Nature, Paris, France). Different feathers of the same peacocks were used in Weiss and Kirchner (submitted for publication) and the present research. Feathers were stored at 24 °C in a laboratory environment of 45% rel. humidity before testing. Small angle X-ray scattering (SAXS) measurements were performed with Cu K_α radiation from a rotating anode generator (Nanostar, BRUKER AXS) equipped with a pinhole camera and an area detector (VANTEC 2000). The samples were mechanically cleaned from the medulla foam, cut into stripes of about 4 cm in length and single strips were measured at a sample-to-detector distance of 14 cm. The exposure time for each pattern was 1800 s and the beam diameter at the sample was 0.5 mm. The distance of the measured spots was reduced to 5 mm for the piece close to the calamus for higher positional resolution. The SAXS intensity patterns were averaged to obtain the scattering intensity $I(q)$, where $q = (4\pi/\lambda)\sin\theta$ is the scattering vector, 2θ the angle between incident and diffracted beam, and $\lambda = 0.1542$ nm the X-ray wavelength. Precisely, the two-dimensional X-ray patterns were evaluated according to the inserts in Fig. 3, left image: for the lateral (equatorial) and the axial (meridional) reflections, the intensity was projected to the respective axes (q_x in equatorial direction, q_z in meridional direction, where the latter coincides with the long axis of the filament and the length of the rachis). To determine the intensity distribution with respect to the azimuthal angle χ, the 2D-patterns were integrated in the regime of each of the reflections, respectively. Background correction was performed by integrating the same regions without sample, subtracting these integrated intensities and taking into account the absorption of the respective sample. The intensities of the reflections were fitted with Gaussian functions to determine the maxima and the half-widths in reciprocal space and then converted into distances and distributions in real space. Differently, for the intersheet distance/interchain distance reflection, the center of gravity of the peak was evaluated, as the shape of the reflection was more rectangular than Gaussian.

Four reflections of the diffraction patterns exemplarily shown in Fig. 3 were evaluated:

(A) The axial reflection of the fourth layer line. It corresponds to the length of the repeating units, about 9.5 nm, which is the pitch of the helix.
(B) The first lateral (equatorial) reflection. It corresponds to the distance between packed filaments.
(C) The intense axial reflection from the 10th layer line. From its splitting the approximate radius of the helix can be determined by searching for the first maximum of the appropriate Bessel function (Harford and Squire, 1997) $J_n(2\pi Q r_{cyl})$. Q is the position of the maximum in reciprocal space and r_{cyl} the radius of the cylinder. The order n of the Bessel function, $n = 2$, follows from the selection rule for feather keratin

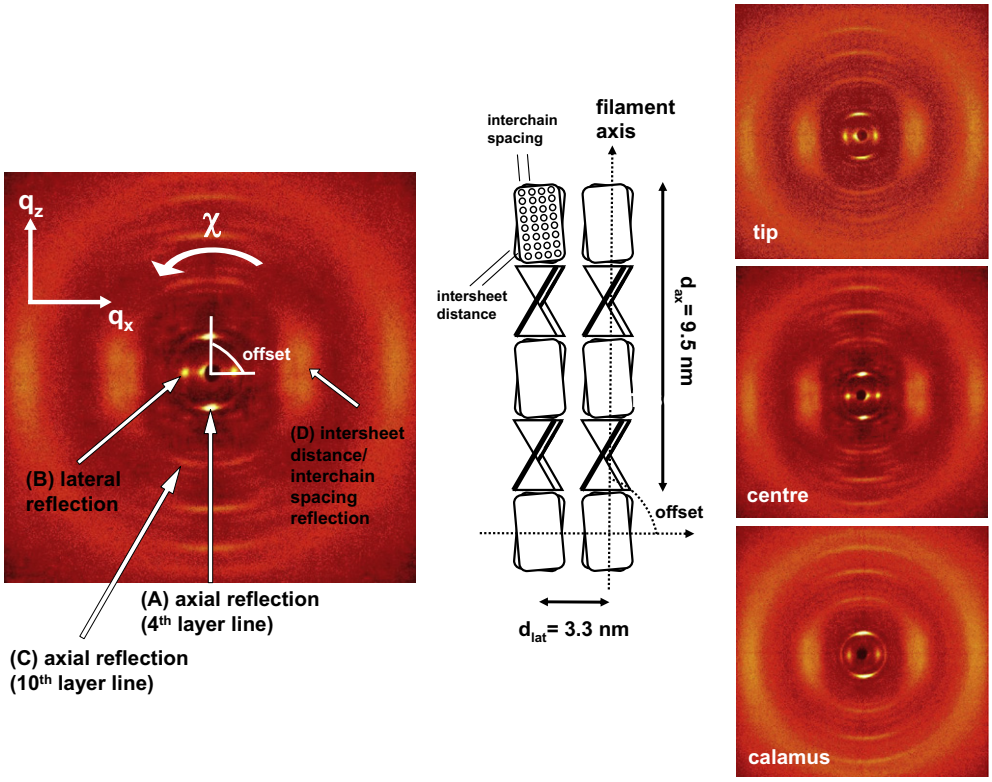

Fig. 3. The four reflections analyzed, (A), (B), (C), (D), are indicated on a typical diffraction pattern, left image. Corresponding real space arrangement proposed by Fraser and Parry (1996) for avian keratin is visible in the center. Right images, three typical scattering patterns along the length of a white peacock feather, from the regions close to the calamus, the center and close to the tip.

($l = n + 4$ m, Fraser et al., 1971, with $l = 10$ being the layer line index, for possible integers n and m). Fraser et al. (1971) observed that this reflection is absent in keratin denaturated by steam; they attributed it therefore to the outer parts of the molecule, which are less stable than the central crystalline beta-core.

(D) The broad equatorial peak. It was attributed to the interchain distance (Schor and Krimm, 1961a) or the intersheet distance (Fraser et al., 1971). We follow here the latter interpretation, evaluated the center of gravity Q of this reflection and converted it to a radius r_{core} by using the second maximum of the Bessel function of zero order, $J_o(2\pi Q r_{core})$. The intersheet distance is then twice this value, 2 r_{core}.

The justification to use two different radii for the structure, r_{core} and r_{cyl}, is that (Fraser et al., 1971) observed the 10th reflection only in the native, unsteamed keratin. As mentioned above, they argued that it stems from the outer parts of the molecule, as the pleated sheet portions of the molecule are more resistant to denaturation due to the regular two-dimensional arrays of hydrogen bonds. The two different radii correspond therefore to the radius of the crystalline beta-core and the outer parts of the molecule, respectively (Fraser et al., 1971).

For clarity the evaluated reflections (A), (B), (C), (D) as well as the offset angle between the axial and the lateral reflection are marked in the left part of Fig. 3. The central part shows the distances in real space inserted into the structure proposed by Fraser and Parry (1996). All error bars in Figs. 4–8 are the sum of fit errors and the positional uncertainty (the finite sample thickness divided through sample-to-detector distance). Errors of wavelength and detector resolution were neglected, as they are either small or do not shift the maximum of the peaks considerably.

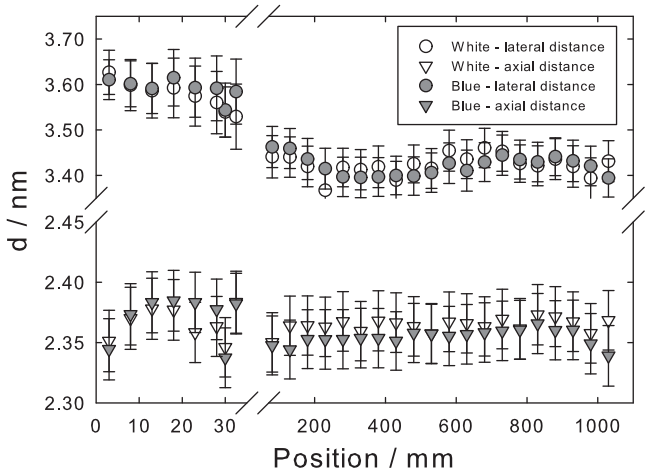

Fig. 4. Positional change of the axial fourth layer line reflection (A – triangles) and the first lateral reflection (B – circles) along the length of the rachis of the feather: open symbols, white peacock, gray symbols, blue peacock. Note that the abscissa is broken to allow for the strong change in the region close to the calamus, positions 0–30 mm.

3. Results

Three examples of scattering images are shown at the right of Fig. 3. These are for the white peacock, one from the region close to the calamus, one in the center and one close to the tip of the feather. The images clearly show the higher orientation with respect to the filament axis in the center region (which covers most of the feather's length), as the azimuthal spread of these reflections is significantly smaller. Evaluation of the axial (A) and the lateral

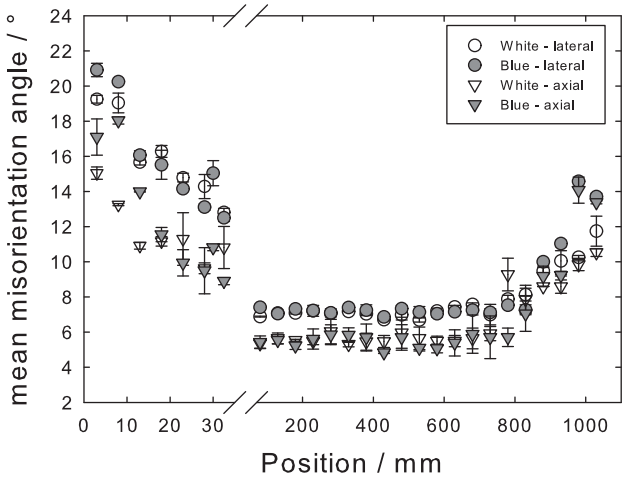

Fig. 5. Mean misorientation angle along the length of the feather, i.e. the Gaussian half-width of the azimuthal spread of the axial reflection from the axial fourth layer line, (A – triangles), and the first lateral reflection, (B – circles). Open symbols, white peacock, gray symbols, blue peacock. The abscissa is broken to allow for the strong change in the region close to the calamus, positions 0–30 mm.

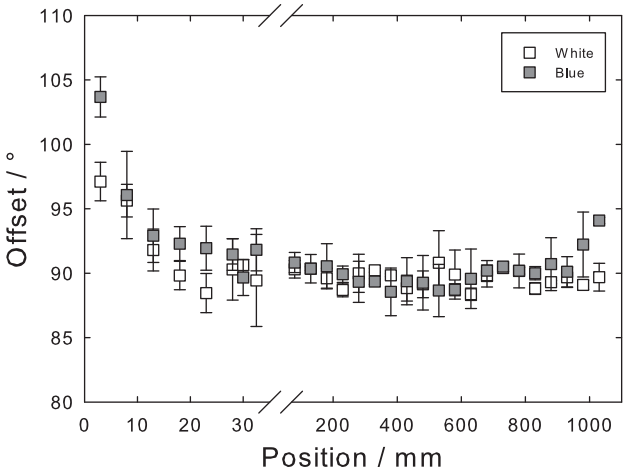

Fig. 6. Offset angle between the axial reflection (A) (length direction of keratin filament) and the lateral reflection (B) (perpendicular direction of the keratin filament). Open symbols, white peacock, gray symbols, blue peacock. The abscissa is broken to allow for the strong change in the region close to the calamus, positions 0–30 mm.

reflection (B) leads to Fig. 4: the triangles, the distances in axial direction, are obtained from the 4th layer line (A). Four times this value is the length of the repeating unit of about 9.5 nm. The lateral packing (circles) is obtained from the lateral reflection (B). Gray symbols are for the blue, open symbols for the white peacock. The abscissa is divided into two parts to allow for the strong change in the region close to the calamus. The ordinate has two separate regions for the respective reflections. The lateral packing distance decreases over the first 50 mm from the calamus, whereas the axial distance first increases and then decreases again. This means that the pitch of the helical structure increases first and then decreases, whereas concomitantly the lateral distance in the perpendicular direction continuously shrinks.

Fig. 5 shows the mean misorientation angle (the intensity spread of the reflection with respect to the azimuthal angle χ, described by the Gaussian half-width) for the axial (A) and lateral (B) reflections. Their cause is the misorientation between keratin filaments and rachis axis. Over the first 50 mm the misorientation angle of the structure decreases, but remains unchanged for most of

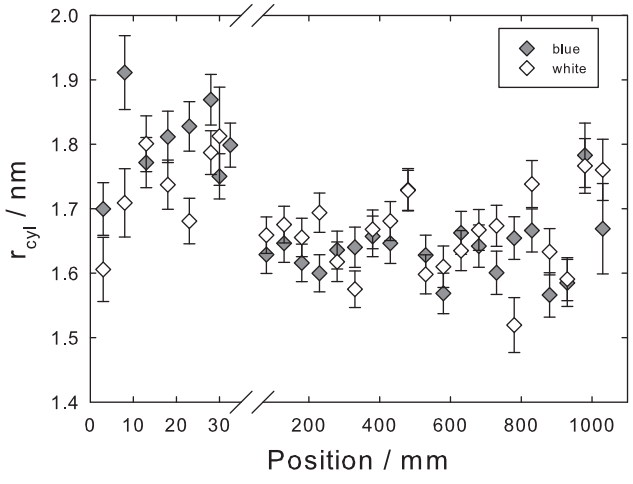

Fig. 7. Cylinder radius evaluated from the axial 10th layer line (C). Open symbols, white peacock, gray symbols, blue peacock. Note the expanded scale near the calamus, positions 0–30 mm.

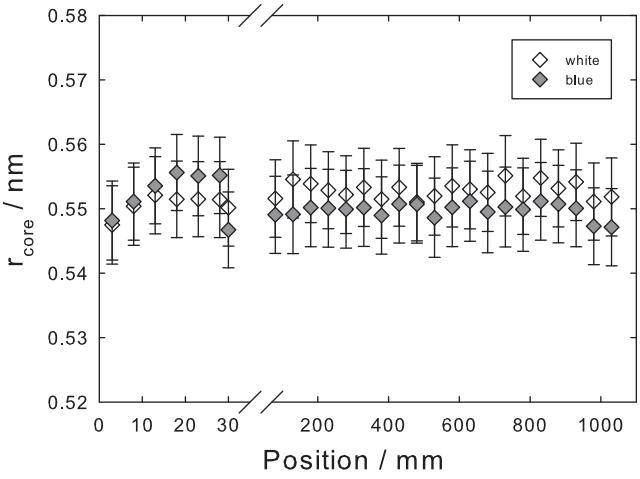

Fig. 8. Core radius r_{core} (half the value of the intersheet distance) from the broad lateral reflection (D). Open symbols, white peacock, gray symbols, blue peacock. Note the expanded scale near the calamus, positions 0–30 mm.

the length, between 30 and 800 mm. Near the tip, the half-widths increase again. The spread in the azimuthal angle (B) is mainly controlled by the mosaicity of the structure. This suggests that the two strands forming the helix increasingly align with the filament and rachis axis and form a highly oriented structure beyond about 50 mm from the calamus.

Another significant change concerns the angle between the first axial (A) and lateral (B) reflections, Fig. 6. It stems from the orientation of the keratin filaments along the long and the perpendicular axis, respectively. The angle strongly decreases over the first 50 mm of the rachis, beyond it remains constant at a value of 90°. This clearly indicates that the arrangement of the filaments at first is not perpendicular to their long axis, but differently inclined, until the length axis of the filament is perfectly perpendicular to their arrangement in the lateral direction.

Due to the helical structure, the 10th layer line (C) is split. From the distance between the maxima an approximate radius of the cylindrical helix can be found by searching for the maximum of the appropriate Bessel function (Harford and Squire, 1997). Fig. 7 shows this cylinder radius r_{cyl} along the length of the feather evaluated from the 10th layer line. It first increases and then decreases to a final value of r_{cyl} = 1.6 nm, where twice this value – the cylin-

der diameter – is slightly smaller than the cylinder distance from the first lateral reflection (Fig. 3).

The core radius r_{core}, where twice this value is the intersheet distance, was obtained from the diffuse and broad lateral reflection (D) and is shown in Fig. 8, also by searching the corresponding maximum of the appropriate Bessel function as described in the Section 2. It is constant along the whole length of the rachis. The alternative interpretation as interchain distance (Schor and Krimm, 1961a) leads to the same conclusion that the crystalline core beta structure is nearly identical over the whole length of the rachis.

4. Discussion

The X-ray diffraction data show that over the 50 mm close to the calamus the degree of order increases, but the final stable structure is only reached beyond this point. In particular, a significant shrinkage of the cylinder radius from 1.8 to 1.6 nm is observed (Fig. 7). This is consistent with the shrinkage of the lateral distance between filaments to approximately 3.4 nm, roughly twice the value of the cylinder radius of the filaments (Fig. 4, circles). Simultaneously, an orientational change of the filaments from an obtuse angle to a perfect perpendicular geometry is observed (Fig. 6). Also the misorientation angle of the filaments with respect to the length axis of the rachis decreases considerably (Fig. 5). However, only a small decrease of only 1% of the length of the repeat unit (the pitch of the helix in axial direction) was observed (Fig. 4, triangles). The pitch, which is four times the *d*-spacing of the fourth layer line, is 9.5 nm and agrees well with the value measured in seagull feather keratin (Fraser et al., 1971). Likewise, the intersheet distance (twice the value of r_{core}, Fig. 8) remains also nearly constant.

For the structural development we propose therefore the model of Fig. 9: during growth, the pairs of β-sheets forming the filament are already present, but their initial orientation with respect to the helix is not well fixed over the first 50 mm from the calamus. Beyond they fall into a highly aligned and oriented structure. The half-widths of both the axial and lateral reflections decrease. The strong increase in alignment is accompanied by only a small shortening of the axial repeat unit, and no change of the intersheet distance. This leads to the conclusion that topologically the crystalline beta structure of the strands is formed early on. Only some small rotations are needed to fix the structure in a zip-like mechanism, where the sidechains perfectly interleave along the filament axis (Fraser and Parry, 2008). The high concentration of hydrophobic residues between the two strands and their interaction is important for the assembly process. They stabilize the final structure (Fraser and Parry, 2008).

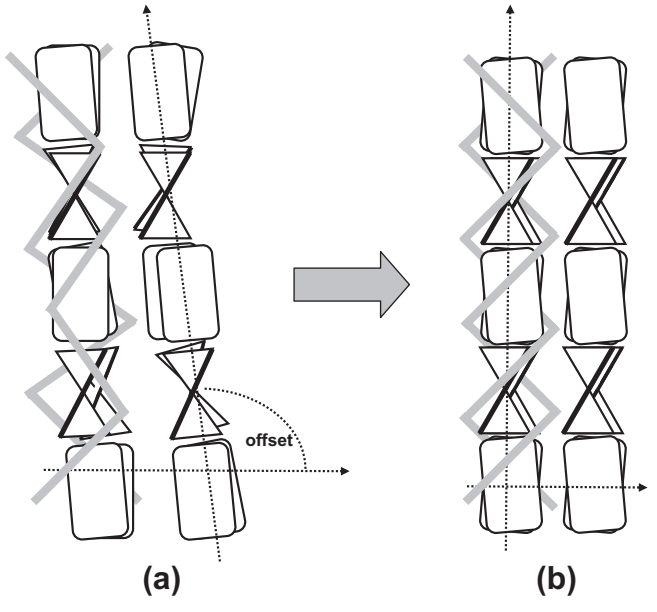

Fig. 9. Structural change from the calamus to the central region: close to the calamus, (a), the β-sheets are misoriented with respect to the filament axis. Away from the calamus, (b), they are increasingly aligned and form a highly oriented structure with filament axis and lateral packing being perfectly perpendicular. The grey bars symbolize the outer parts of the molecule, which are not organized in pleated sheets. Both the diameter of the filaments and their distance decreases.

The main shrinkage appears in the so-called "matrix", the portion of the molecule not forming the core beta structure. It may be speculated that these outer portions of the molecule, 67 of 98 amino acids, surround the crystalline core beta structure and lead to a contraction of the structure as a whole. Since the shrinkage is deduced from the 10th layer line (C), known to be sensitive to denaturation (Fraser et al., 1971), we suspect that it can be attributed to the end parts of the molecule. The 10% "matrix" shrinkage is accompanied by a change of the offset angle between the filament axis and the lateral packing of the filaments. It changes from 100° to 90° within the first 50 mm from the calamus. One can imagine a structure with a hard and stiff crystalline core of 31 amino acids (3.3 kDa) wrapped into the 67 amino acids (6.5 kDa) of the tails.

5. Conclusions

The structural development of the keratin filament within a peacock's feather is studied by X-ray diffraction along the length of the feather, from the calamus to the tip, where the eyes are located. The structure changes considerably over the first 50 mm and then remains constant over almost the total length (1 m) of the feather. Close to the tip, the structure loses its high crystallinity, probably because there the cortex function ceases to be mechanical, but serves to organize the optical eye patterns. We propose an explanation based on structural models in the literature (Fraser and Parry, 1996, 2008; Fraser et al., 1971). Whereas the crystalline core is nearly unchanged (first a small increase and then a decrease of the helical pitch), the distance between neighboring filaments decreases significantly. Concomitantly, the cylinder radius decreases if evaluated from the 10th layer line, which is nearly absent in denaturated keratin. This leads to the interpretation that the inner crystalline core is very stable, whereas the outer portions of the molecule possibly surround the inner core and stabilize the structure as a whole. Concomitantly with the shrinkage, also visible by the decrease of the distance between the filaments, the angle between the filament axis and the lateral packing approaches the perfect perpendicular arrangement of 90°. It may be speculated that this structure resembles stiff columns built up from small crystallographic units, which are joined together and stabilized by the tails of the molecules wrapped around them, the "matrix". This might increase the bending resistance of the structure. Finally, it is worth noting that for quill embroidery (Weiss and Kirchner, 2010) artisans use only strips cut from the central part (30–80 cm) of the feather.

Acknowledgments

The support from the Austrian Science Fund (FWF), Proj. nr. P20693, is gratefully acknowledged. I.M.W. and H.O.K.K. thank Eduard Arzt for his continuing support.

References

Alexander, D.E., Gong, E., Martin, L.D., Burnham, D.A., Falk, A.R., 2010. Model tests of gliding with different hindwing configurations in the four-winged dromaeosaurid Microraptor gui. PNAS 107, 2972–2976.

Astbury, W.T., Beighton, E., 1961. Structure of feather keratin. Nature 191, 171–173.
Astbury, W.T., Marwick, T.C., 1932. X-ray interpretation of the molecular structure of feather keratin. Nature 130, 309–310.
Astbury, W.T., Woods, H.J., 1934. X-ray studies of the structure of hair, wool, and related fibres. II. The molecular structure and elastic properties of hair keratin. Philosophical Transactions of the Royal Society of London, Series A 232, 333–394.
Benton, M.J., 2010. Evolutionary biology: new take on the red queen. Nature 463, 306–307.
Busson, B., Engstrom, P., Doucet, J., 1999. Existence of various structural zones in keratinous tissues revealed by X-ray microdiffraction. Journal of Synchrotron Radiation 6, 1021–1030.
Cameron, G.J., Wess, T.J., Bonser, R.H.C., 2003. Young's modulus varies with differential orientation of keratin in feathers. Journal of Structural Biology 143, 118–123.
Dalla Valle, L., Nardi, A., Belvedere, P., Toni, M., Alibardi, L., 2007. β-Keratins of differentiating epidermis of snake comprise glycine–proline–serine-rich proteins with an avian-like gene organization. Developmental Dynamics 236, 1939–1953.
Eckhart, L., Valle, L.D., Jaeger, K., Ballaun, C., Szabo, S., Nardi, A., Buchberger, M., Hermann, M., Alibardi, L., Tschachler, E., 2008. Identification of reptilian genes encoding hair keratin-like proteins suggests a new scenario for the evolutionary origin of hair. PNAS 105, 18419–18423.
Fraser, R.D.B., Parry, D.A.D., 1996. The molecular structure of reptilian keratin. International Journal of Biological Macromolecules 19, 207–211.
Fraser, R.D.B., Parry, D.A.D., 2008. Molecular packing in the feather keratin filament. Journal of Structural Biology 162, 1–13.
Fraser, R.D.B., MacRae, T.P., Parry, D.A.D., Suzuki, E., 1971. The structure of feather keratin. Polymer 12, 35–56.
Harford, J., Squire, J., 1997. Time-resolved diffraction studies of muscle using synchrotron radiation. Reports on Progress in Physics 60, 1723–1787.
O'Donnell, I.J., Inglis, A.S., 1974. Amino acid sequence of a feather keratin from silver gull (*Larus novae-hollandiae*) and comparison with one from emu (*Dromaius novae-hollandiae*). Australian Journal of Biological Sciences 27, 369–382.
Ruben, J., 2010. Paleobiology and the origins of avian flight. PNAS 107, 2733–2734.
Schor, R., Krimm, S., 1961a. Studies on the structure of feather keratin: I. X-ray diffraction studies and other experimental data. Biophysical Journal 1, 467–487.
Schor, R., Krimm, S., 1961b. Studies on the structure of feather keratin: II. A [beta]-helix model for the structure of feather keratin. Biophysical Journal 1, 489–515.
Stone, R., 2010. Bird-dinosaur link firmed up, and in brilliant technicolor. Science 327, 508.
Sullivan, C., D.W.E. Hone, X. Xu, and F. Zhang, 2010. The asymmetry of the carpal joint and the evolution of wing folding in maniraptoran theropod dinosaurs. Proceedings of the Royal Society of London, Series B [epub ahead of print].
Weiss, I.M., Kirchner, H.O.K., 2010. Quill embroidery: a case study in the mechanics of biological materials. Advanced Engineering Materials 12, 412–416.
Weiss, I.M., Kirchner, H.O.K., submitted for publication. The peacock's train (*Pavo cristatus* and *Pavo cristatus* mut. alba) I. Structure, mechanics, and chemistry of the tail feather coverts. Journal of Experimental Zoology.